The Ambiguity of Celestial Dynamics

Alfred N. van Hoek

Formerly: Department of Neurology, University of Utah, 36 South Wasatch Drive, SMBB 4322, Salt Lake City, UT 84112-5001.
E-mail: alfred.vanhoek@hsc.utah.edu; vanhoek@mac.com. ORCID 0000-0003-2724-6855.

Since the discovery of stellar aberration, human perception failed to recognize the fundamental property of motion parallax to recover the depth of the universe. Stellar aberration, the motion of the fixed stars in the perceived direction of Earth's motion, is the essence of reversed perspective [Purves D., Andrews T. J. *Proc. Natl. Acad. Sci. USA*, 1997, v. 94, 6517–6522]. The true-to-reality perception requires a finite-radius celestial sphere, which functions as a non-inertial frame of reference; its coordinates along the line-of-sight describe a Coriolis circulation at a parallax distance of 58.13 light-days.

1 Introduction

The perception of a three-dimensional universe projected onto a two-dimensional projection surface of the celestial sphere is or becomes equivocal, because the uncertainty [1] requires the distinction between illusion and veridicality. The recovery of the missing third dimension, the depth of field is prone to these two possibilities and may be best described by the Necker illusion [1], which switches between proximal and distal faces of a two dimensional representation of a cube. The spatial relationship of the proximal and distal faces can be ascertained by motion parallax so that the object moves laterally in relation to the background, thereby providing perspective or true-to-reality perception [1]. The illusionary perception, the distal and proximal faces of the cube are perceived to be front, respectively, back, associates with reversed perspective and motion parallax fails; the background appears to rotate in the direction of motion. When considering celestial sphere grids at a finite and at an infinite distance, the motion of Earth around the Sun will cause parallax of the proximal grid in annual fashion with respect to the fixed stars. However, perceiving the sphere surface as the distal grid, the motion of the Earth will cause negative parallax of the stars, which is known as stellar aberration [2]. Special relativity proposed that space contraction in the direction of motion is a logical consequence of the universal constant, the finite speed of light. Among other laws of motion, it proclaimed the law of stellar aberration [3], which as it stands is incompatible with the finite-radius celestial sphere. To discern illusion from reality, we address the intricacy of celestial sphere radii (finite or infinite) in this thesis.

2 Celestial sphere considerations

The nature of a celestial sphere centered on Earth with a fixed orientation (Fig. 1) and the apparent alignment with the fixed stars suggests a stationary frame of reference. However, the discovery of stellar aberration in the direction of Earth's motion was a surprising phenomenon because a fixed point at the firmament should not cause any measurable displacement. Mathematically, centering the celestial sphere to Earth or to an arbitrary planet in a fixed configuration, as shown in Fig. 1, two rotational frame of references need to be reconciled with. The anti-clockwise planetary orbit drives the celestial sphere into rigid body circulation, subjecting the coordinates, emanating from the centre towards the surface of the sphere along the spindles, to the nonzero curl of the velocity field $\mathbf{u}$,

$$\boldsymbol{\xi} = \nabla \times \mathbf{u}, \tag{1}$$

also known as the vorticity $\boldsymbol{\xi}$. Because the rotation occurs in the x-y plane, the vertical component ζ is nontrivial,

$$\zeta = \frac{\partial v}{\partial x} - \frac{\partial u}{\partial y}, \tag{2}$$

where u and v are the velocity components of the planetary orbital velocity $\Omega \times R$, i.e.

$$\begin{aligned} u &= -\Omega y\, \hat{\mathbf{x}} \\ v &= \Omega x\, \hat{\mathbf{y}}. \end{aligned} \tag{3}$$

Substitution of (3) into (2) leads to the identity

$$\zeta = 2\Omega. \tag{4}$$

This means that the unit vectors $\hat{\mathbf{x}}$, $\hat{\mathbf{y}}$, $\hat{\mathbf{z}}$ (Fig. 1, left panel) are locked to the orbital period of the planet, i.e, the vector $\hat{\mathbf{x}}$ is facing the rotational axis Ω. To steady the sphere in a fixed orientation requires a clockwise turning about its centre, which orients it in the stationary position (Fig. 1, right panel). This clockwise turning does not nullify the vorticity field of planetary motion, defining the celestial sphere system as a non-inertial frame of reference. Fig. 2A is a graphical representation of a celestial sphere centered on the planet with radial distance equal to the orbital radius of the planet. An arbitrary spindle, from the centre of the planet to the surface of the sphere, marked as 1-1, 2-2, 3-3, 4-4, 5-5 (Fig. 2A), represents the fixed line-of-sight towards the firmament and will describe an anti-clockwise circular trajectory. Divergent light-rays (exemplified in Figs. 2A, 2B) from a star to a receiver become convergent lines from receiver to the source as if they are parallel lines that vanish in perspective (Fig. 2A,

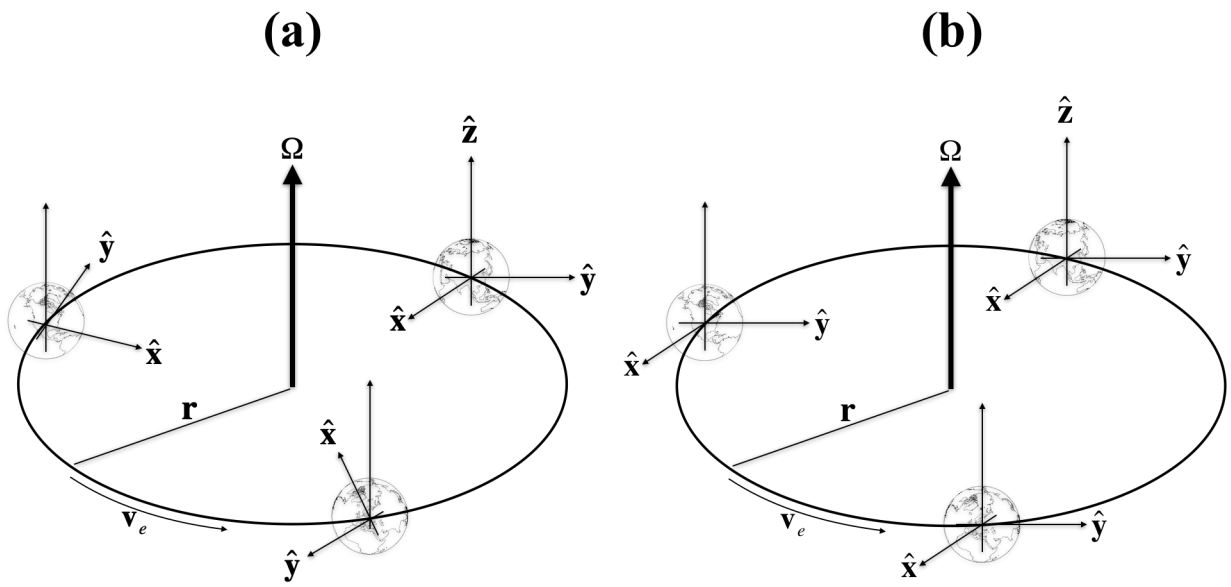

Fig. 1: **Coordinate systems.** An orbiting coordinate system around the stationary Sun is period locked (a).The unit vectors maintain a fixed orientation (b) by the clockwise annual spin of the celestial sphere about its axis $\hat{\mathbf{z}}$ to oppose the counterclockwise spin-orbit locking about Ω. The origin of the celestial sphere moves at constant angular velocity about the axis Ω with a fixed distance $\mathbf{r}$ from the centre of an inertial frame of reference.

2B), which also should hold when the light rays are truly parallel. This contrasts the divergent spindles of the celestial sphere that never can become parallel and cannot vanish in perspective as true parallel lines do*. Thus, with respect to the spindle of the celestial sphere, the direction to a star changes, forming different angles with the chosen spindle. The orbital trajectory of a spindle occurs further out in space when the radius of the celestial sphere is increased. The completion of a full planetary orbit of the sphere results in an imaginary Lissajous figure that is produced by a hula-hoop mechanism of the celestial sphere. The width of the donut-shaped Lissajous equals the diameter of the planetary orbit. This imaginary orbit, composed by the time-dependent endpoint of a single spindle, is thus formed by a bundle of parallel lines (Fig. 2C). If the radial distance of the spindle is increased we should expect the imaginary orbit to vanish in perspective. But the angling of the telescope as observed [2] appears to be a requirement to adjust the celestial sphere coordinate system to steady the stars [this thesis], suggesting a finite-radius celestial sphere. We then could conclude, from whatever direction observations are made, that the velocity field of a planet creates an imaginary orbit of a coordinate spindle about a star representing the Sun. The imaginary Sun is then, alike the endpoint of the celestial sphere spindle, located at the celestial sphere surface, exemplifying the imaginary Sun-Earth orbit system at a finite distance. This "kinematic optical" effect at a distance, the frame-dependent Coriolis circulation, is what aberration of light may represent and could be an equivalent to Snell's law.

*Infiniteness of the celestial sphere is usually interpreted as if the spindles are parallel lines. It then may be practical given the centre of the celestial sphere would be everywhere [5].

3 The finite-radius celestial sphere

Figs. 3A and 3B highlight the angling necessary to maintain the line-of-sight towards the perceived stationary imaginary Sun Q in the ecliptic and pole directions, respectively. The line-of-sight coincides with a spindle of the celestial sphere and as shown the color coded circle and matching color-coded spindle/radius defines the line EQ with length C, and is equal to the centre-to-centre distance of the imaginary orbit and its planetary orbit. Since the line-of-sight can be chosen at will towards a star or an invisible point of interest, the angling towards Q in the figures, is caused by the changing position of the celestial sphere anchored to the orbital motion around the Sun. The fixed distance C, i.e. EQ, suggests (Fig. 4) the Scotch yoke reciprocating motion where the orbital position of the planet, point E, changes the position of the centre of the celestial sphere with respect to point Q (cf. Fig. 3). From the viewpoint of O, Q will slide along the vertical axis that coincides with the line OQ. According to the cosine rule, we have

$$(EQ)^2 = (OE)^2 + (OQ)^2 - 2 \cdot OE \cdot OQ \cdot \cos\theta\,,$$

$$(OE)^2 = (EQ)^2 + (OQ)^2 - 2 \cdot EQ \cdot OQ \cdot \cos\phi\,,$$

where EQ is the equivalent of the crank rod length equaling C and OE represents the orbital radius R. Substitution of the

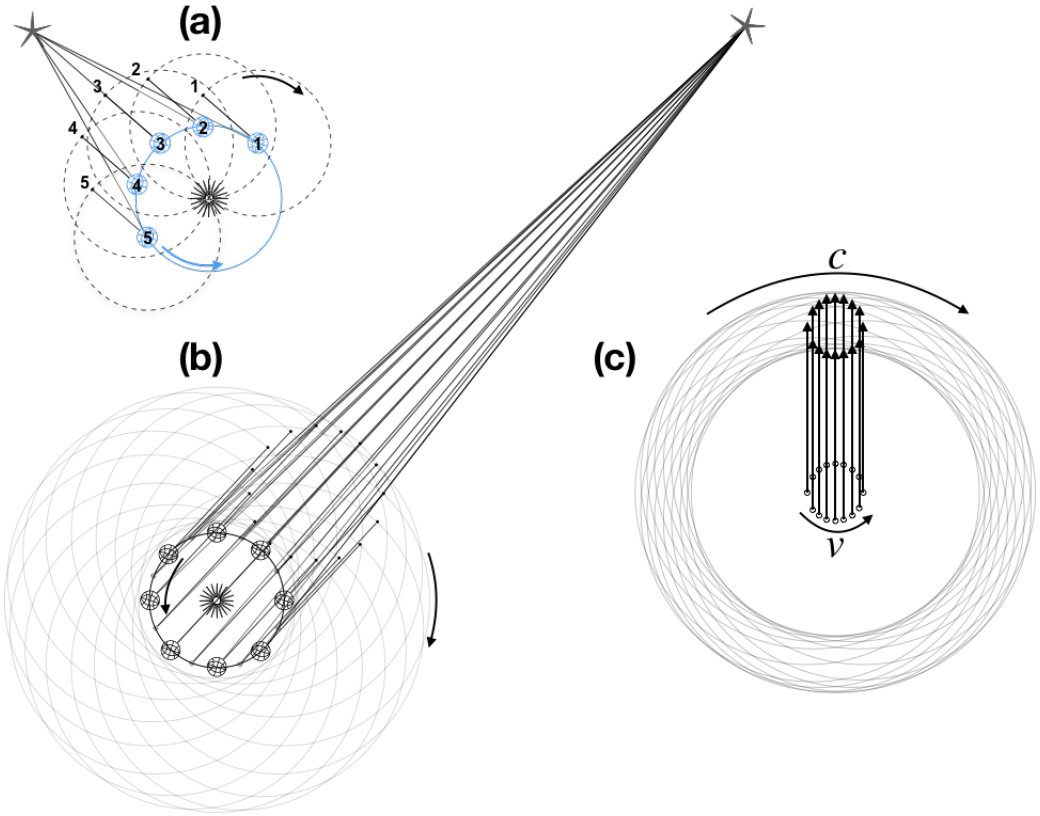

Fig. 2: **Celestial sphere radius and the velocity field.** Views of a planetary body rotating in a stationary frame of reference with the Sun as its centre. The celestial sphere centered on the planet with the same radius as the orbit (a) has a fixed orientation. The spindle of the celestial sphere at positions 1 trough 5 does not change in direction, while the direction to a star is dependent on the orbital motion of the planet. The increase of the celestial sphere radius (b) and (c) reduces the angling to a star at a finite distance. The line-of-sight to the surface of the celestial sphere (c) describes a circulation with the radius equal to the orbital radius. In perspective the subtended angle is equal to the parallax angle. To keep the celestial sphere in a fixed orientation, the axial clockwise rotation opposes the counterclockwise orbital motion of the celestial sphere. At the parallax distance the orbital velocity of the sphere surface is equal to the speed of light.

first cosine formula into the second cosine formula, replacing $(EQ)^2$, yields

$$OQ = R\cos\theta + C\cos\phi, \tag{5}$$

where OQ represents the projection of the lines R and C with respect to the stationary reference frame of the Sun. The first term at the right hand side is the offset of point Q with respect to the Sun, caused by orbital motion. The second term at the right hand side describes the radial component of stellar aberration. The law of sines,

$$R\sin\theta = C\sin\phi, \tag{6}$$

corresponds to the tangential component of stellar aberration. Substitution of (6) into (5) provides the combined form, independent of the subtending angle ϕ term, where the angle θ equals the angular velocity $\dot{\theta}$ of the planet at time t, yielding

$$OQ = R\cos\theta + \sqrt{C^2 - R^2\sin^2\theta}. \tag{7}$$

Motion of point Q away or towards the Sun is the quintessence of the hula-hoop motion of the celestial sphere (Fig. 2 and 3), contributing to the decreasing and increasing parallax angle ϕ, when observing aberration in the direction of the plane of the ecliptic. The second term at the right hand side of (7), normalized to C,

$$\cos\phi = \sqrt{1 - \frac{R^2}{C^2}\sin^2\theta}, \tag{8}$$

is complementary to (6). In terms of v and c, multiplying the radii R and C with the planetary angular velocity $v = \Omega \times R$ and $c = \Omega \times C$, the identities $vc^{-1} = \beta = RC^{-1}$ modify the above sine and cosine of ϕ (Eqs. 6, 8) to

$$\sin\phi = \beta\sin\theta \tag{9}$$

and

$$\cos\phi = \sqrt{1 - \beta^2\sin^2\theta}. \tag{10}$$

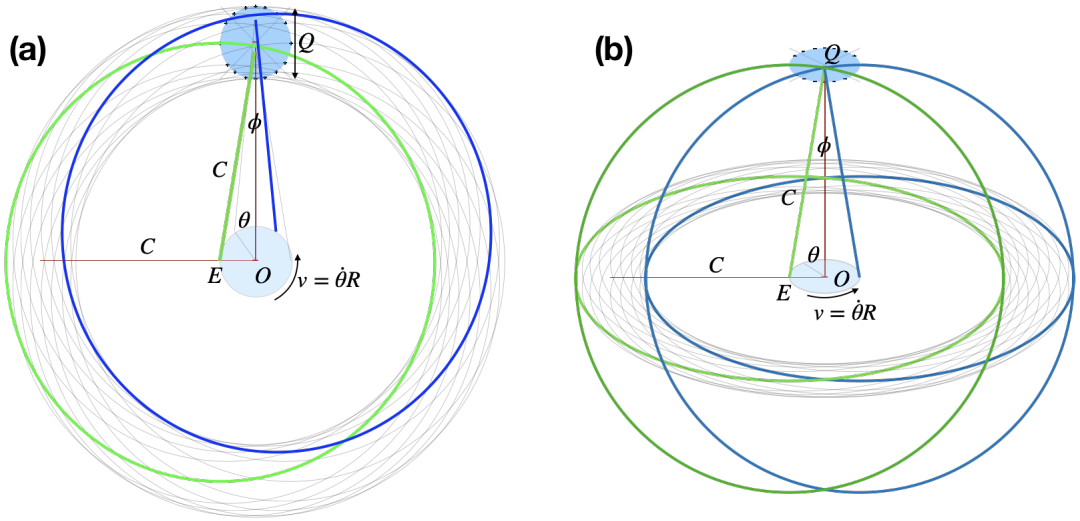

Fig. 3: **Geometry of negative parallax.** Point O represents the Sun and E is the position of the Earth in its orbit. Earth is the centre of the celestial sphere, the light blue circle is the Earth orbital plane and the dark blue filled circle is the traced-out orbital path of the Earth at distance C. (a): geometry of the celestial sphere in the ecliptic plane. (b): geometry of the celestial sphere towards the poles of the sphere.

Eq. (9) is reminiscent of the formula used to describe Snell's law, when referring to light or other waves passing through a boundary, which would be the celestial sphere surface that has a tangential velocity equal to the luminal speed c (Fig. 2C). The spindle EQ (Fig. 4) is the line-of-sight to and coincides with a light ray from the faraway fixed star of interest. The flight time of light from Q to E (see Sections 5 and 6) equals one radian of the orbit and is another property of the "kinematic optical" effect at a distance. The value of the aberration of light is defined when $\theta = \pm 90°$. The Pythagorean (9–10) becomes a right triangle. This condition is also equivalent to the line-of-sight when EQ is perpendicular to the ecliptic. The right triangle in terms of β is a Lorentz triangle with sides $1, \beta$ and $\gamma\beta$, where

$$\begin{aligned} \sin\phi &= \beta, \\ \cos\phi &= \sqrt{1-\beta^2} = \gamma^{-1}. \end{aligned} \tag{11}$$

The cosine term is identical to the reciprocal of the Lorentz gamma factor, i.e. $\gamma = \sec\phi$, which in terms of the special theory scales the Lorentz transformation matrix. Thus, the outcome of this treatise on the fixed and finite celestial sphere radius, leads to the same aberration of stellar light β but with opposite sign. In terms of the three-dimensional universe the stars are no longer perceived illusory and will behave veridically [1].

4 Transformation matrices

The general form of the special case (11), embodied by (9) and (10), also provides novel insight in which motion involves not only a change of β when considering the direction cosine, the line-of-sight, but also a change of the gamma-like factor (10). Given the radial vector $\boldsymbol{r}$ and time t, utilizing (9–10) instead of γ and β (11) as defined and used in the Lorentz transformation matrix [3], premultiplication of the vector $[t, \boldsymbol{r}]$ with the generalized and modified Lorentz transformation matrix containing the vorticity entries, i.e. (9) and (10),

$$\begin{bmatrix} t' \\ \boldsymbol{r}' \end{bmatrix} = \begin{bmatrix} \sec\phi & -c^{-1}\tan\phi \\ -c\tan\phi & \sec\phi \end{bmatrix} \begin{bmatrix} t \\ \boldsymbol{r} \end{bmatrix}, \tag{12}$$

results in

$$t' = \sec\phi\left(t - \boldsymbol{r}c^{-1}\sin\phi\right) \tag{13a}$$

$$\boldsymbol{r}' = \sec\phi\left(\boldsymbol{r} - ct\sin\phi\right). \tag{13b}$$

The derivation of the Lorentz transformation, matrix $\mathbf{L}$ involved the Galilean matrix, $\mathbf{G}$, and an assisting* or temporal matrix, $\mathbf{T}$. In generalized vorticity forms (cf. (12)) they become

$$\mathbf{G}_\odot = \begin{bmatrix} 1 & 0 \\ -c\sin\phi & 1 \end{bmatrix} \tag{14}$$

and

$$\mathbf{T}_\odot = \begin{bmatrix} \cos\phi & -c^{-1}\tan\phi \\ 0 & \sec\phi \end{bmatrix}. \tag{15}$$

Premultiplication of $\mathbf{G}_\odot$ with $\mathbf{T}_\odot$ gives the Lorentz matrix (cf. (12))

$$\mathbf{L}_\odot = \mathbf{T}_\odot\mathbf{G}_\odot. \tag{16}$$

If $\theta = \pm 90°$ (9–10), these matrices reduce to those Einstein derived. The subscript $\odot$ refers to a circular path with the line-of-sight along a spindle of the celestial sphere. Matrix $\mathbf{L}_\odot$ exemplifies the finite speed of light embodied by matrix

*The Lorentz matrix was heralded by the Zeitgeist of thence. The assisting system did not gain significance given its auxiliary status.

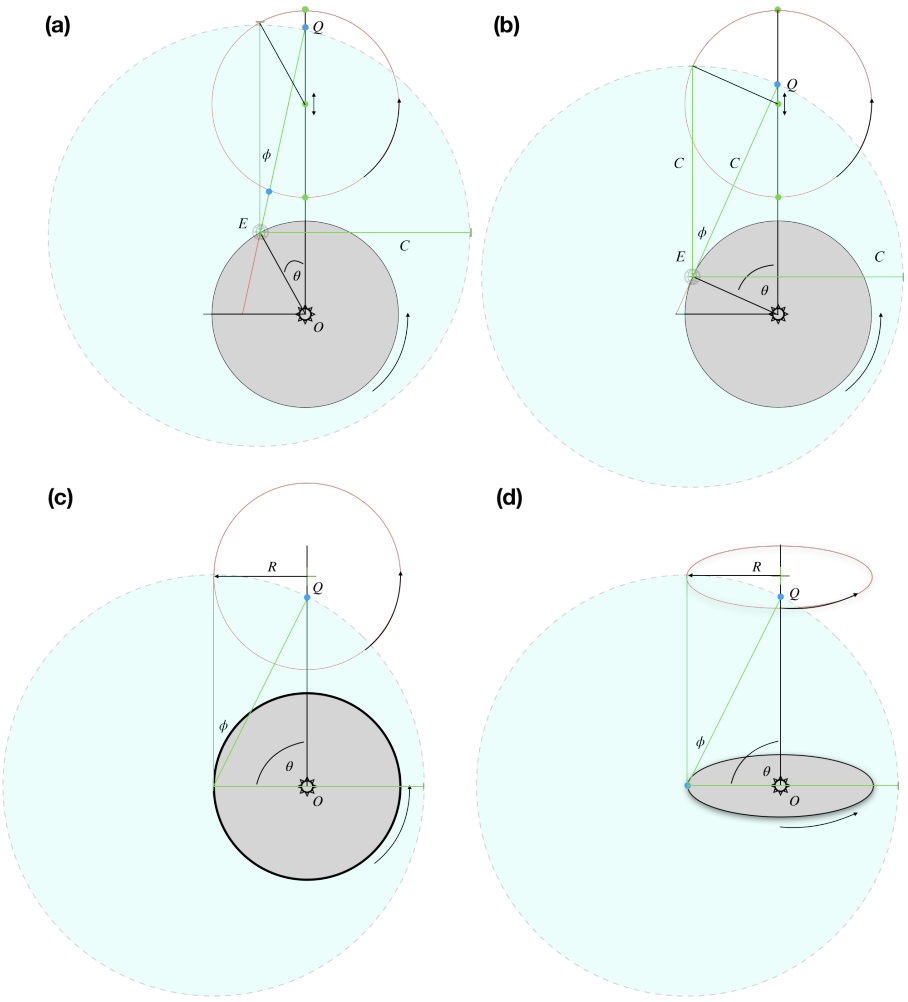

Fig. 4: **Scotch yoke reciprocating motion.** Earth's celestial sphere (light blue) with respect to the origin O, (the Sun) at (a), (b) and (c), affects the position of point Q, which is the imaginary Sun (see Section 2) as seen from Earth, E, sliding it up and down along the vertical line from O to Q. The line EQ is the line-of-sight (a celestial sphere spindle) with a fixed length. A complete revolution of Earth replicates the orbit of Earth (red colored). Earth's celestial sphere at (c) in the equatorial plane is replicated as (d) when the line-of-sight is towards the celestial pole.

$\mathbf{T}_\odot$, exemplifies the invariance of c and $\mathbf{G}_\odot$ exemplifies the Galilean transform. The location of a point in space and time is described by matrix $\mathbf{G}_\odot$; to detect this point by light requires a method, a transformation by using matrix $\mathbf{T}_\odot$. The identities

$$\mathbf{G}_\odot = \mathbf{T}_\odot^{-1}\mathbf{L}_\odot\,, \tag{17a}$$

$$\mathbf{T}_\odot = \mathbf{L}_\odot\mathbf{G}_\odot^{-1}, \tag{17b}$$

constitute a mechanism to transform a light-clock signal originating from a point and defined by matrix $\mathbf{L}_\odot$ to what will be an ordinary light-independent point in space and time defined by matrix $\mathbf{G}_\odot$. The true form of identifying an object is not perceived by light, which confirms Bradley's assessment 300 years ago or in other words these matrices correct for the delay of arrival time of light. The identities (17) suggest to convert light-signal based data to real data allowing ordinary addition of velocities and if necessary use the identity (16) to determine the Doppler effect.

5 The one radian of an orbit

The parallactic displacement of the coordinate system defined by β equaling $vc^{-1} = RC^{-1}$ for each of the planets of the solar system were calculated from their orbital radius R (Table 1, row 1) and period T (Table 1, row 2), yielding β, the radius of the celestial sphere C and the aberration angle $\phi = \arcsin\beta$ (Table 1, row 3). The celestial sphere radii increase with decreasing aberration angle, while the ratio of the celestial sphere radius C and period T of the planetary orbit

$$\frac{C}{T} = \frac{\Omega \times C}{2\pi} = \frac{c}{2\pi} \tag{18}$$

Table 1: The planets of the solar system are listed with their orbital radius R (row 1, [au]), period T (row 2, [year]) and the aberration angle ϕ [arcsec]. The duration of a light signal from the celestial sphere surface to the planet μ^{-1} (row 4, [day]) equals the one radian of the orbit, see (18). Based on the planet-Sun barycentre distance, bc (row 5, [km]), the solar orbit velocity v_{Sun} (row 6, [m/s]) was calculated using the planetary period T. The ratio of solar orbit velocity and the speed of light is provided in terms of an aberration angle ϕ_{bc} (row 7, [arcsec]), representing the planetary-specific celestial sphere of the Sun (see Section 7).

	Mercury	Venus	Earth	Mars	Jupiter	Saturn	Uranus	Neptune
R	0.39	0.72	1	1.52	5.2	9.54	19.2	30.1
T	0.241	0.615	1	1.88	11.9	29.5	84.1	164.8
ϕ	33.19	24.09	20.49	16.6	8.99	6.64	4.68	3.74
μ^{-1}	14.01	35.75	58.13	109.28	691.75	1,714.83	4,888.73	9,578.82
bc	10	265	445	74	742,465	408,110	12,585	230,609
v_{Sun}	0.007936	0.08577	0.08955	0.007786	12.467	2.759	0.2967	0.2786
ϕ_{bc}	0.000005	0.00006	0.00006	0.000005	0.0086	0.0019	0.0002	0.0002

is a constant, 10 066.61 au/year, i.e. one radian of the orbit, which equals the duration of a light signal from the celestial sphere surface to the centre of Earth – for Earth it is 58.13 days (Table 1, row 4). This value is the reciprocal of the Gaussian gravitational constant confirming planetary-specific finite-radius celestial spheres and aberration angles according to Kepler's third law of planetary motion and Newton's law of gravitation. In terms of β, Kepler's law becomes

$$r_k = \frac{4\pi^2 K}{c^2} = \beta^2 R, \tag{19}$$

where K is Kepler's constant and the radius r_k is half the value of the Schwarzschild radius. Newton's law becomes

$$r_k = \frac{GM}{c^2} = \beta^2 R \tag{20}$$

with G the gravitational constant, and M the mass of the solar system. The value of r_k equals 1476.24711 m. The relation between the Kepler radius (or half the Schwarzschild radius), the parallactic aberration angle and the one radian of an orbit may lead to the concept of discrete radii of the celestial sphere with the vanishing of Earth's imaginary orbit in perspective to infinity, depending on the optical resolution of detection.

6 Multiple discrete stellar aberrations

The one radian of a circle is the equivalent of a phase shift of 1 rad between planetary motion and the arrival time of light from the surface of the celestial sphere, which can be understood from considering the planetary orbit and its imaginary orbit at distance C. Both orbits are in phase, but a light signal requires time to arrive and during the delay the planet travels a curved distance equal to its orbital radius R. This phase difference of 1 rad, noting its association with the radius $C = \beta^{-1}R$ may suggest additional radii $\beta^{-n}R$, because the phase-shift will be precisely 1 rad under these conditions. For Earth, when n equals 2, the flight time of light is a little over 1 602 light-years, i.e. equivalent to 1 602 orbital revolutions. The wobbling (hula hoop) of the celestial sphere traces out the planetary orbit at $\beta^{-1}R$ and $\beta^{-2}R$, and thus, light from ~58 days ago and from ~1 602 years ago are simultaneously observed along the same celestial sphere spindle and in-phase. The vanishing of imaginary planetary orbits at discrete distances in perspective and by virtue of the visibility of the stars by vanishing stellar aberrations (20.49 arcsec, 0.002 arcsec, ...) in perspective is a powerful mechanism to observe depth. Instead of having a celestial sphere with an infinite radius to measure parallactic displacement of stars in the opposite direction of motion, a finite-radius celestial sphere causes negative parallax of all the stars, not some (Fig. 2). Each depth marker on a spindle defines the coordinate at a distance and motion of the observer perpendicular to the line-of-sight does not significantly alter the coordinates at the depth markers faraway with respect to the line-of-sight, in contrast to depth markers nearby. Multiple markers along a spindle and vanishing parallel lines in perspective provide depth perception because the line-of-sight cross spindles when the coordinate system is in motion. The multitude of discrete radii for a given celestial sphere and a fixed line-of-sight along a spindle, i.e. when the telescope is not adjusted, will scan a circular area of the firmament creating a radial field of view of 90° ($\beta^0 = 1$, cf. Fig. 2A), a radial field of view of 20.49 seconds of an arc (β^1, cf. Fig. 2C), a radial field of view of 0.002 seconds of an arc (β^2), a radial field of view of 0.2 microseconds of an arc (β^3), and so on, centered on an imaginary Sun in an anti-clockwise fashion. Large scale rotations suggesting a cosmic web have been reported recently. For example, galaxy rotation appeared to be considerably coherent with the average line-of-sight motion of neighbors at far distances (1–6 Mpc). These rotations are counterclockwise and have a mean velocity at ~30.6 km/s [4], which resembles Earth's orbital velocity. The values reported are consistent

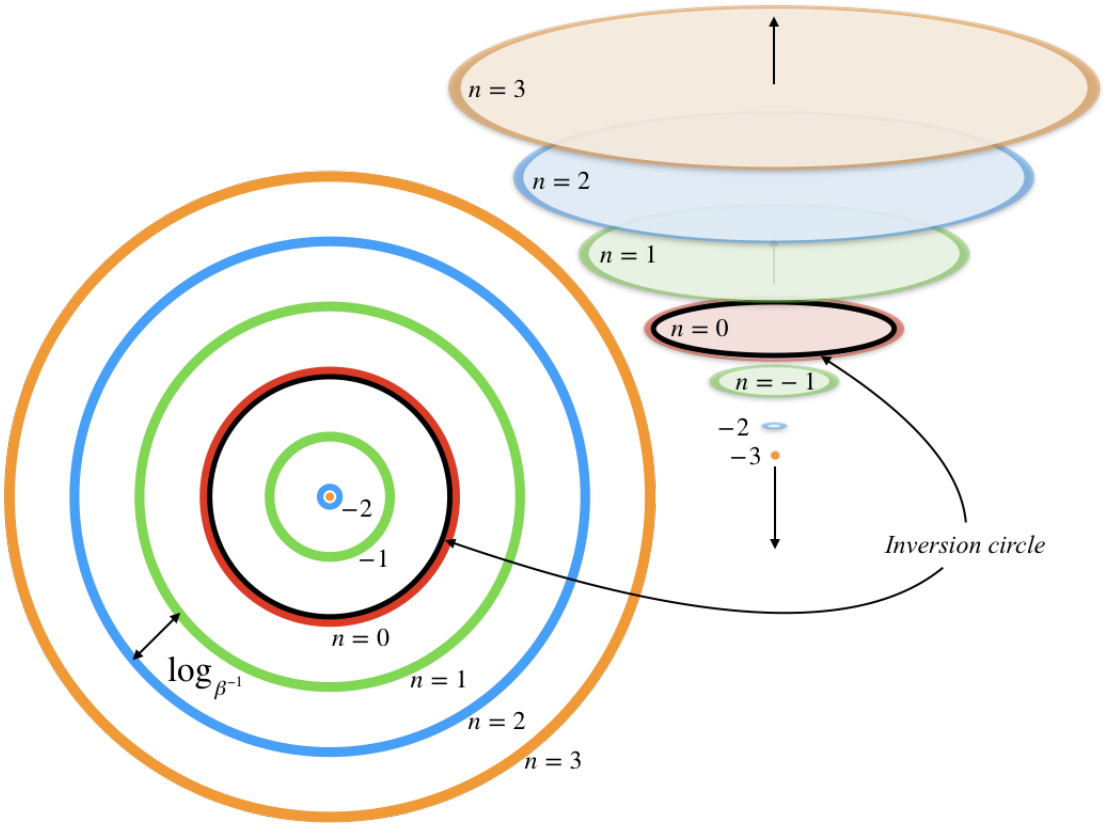

Fig. 5: **Inversion Circle.** The logarithmic scale with base β^{-1} separates the circles (left and right panels). The inversion circle (black) is identical to the planetary orbit (red) when $n = 0$ (24). The green circles represent a circle with radius R/β equal to C when $n = 1$, the principal celestial sphere radius as described in this paper, and its inverse with the inverse radius βR when $n = -1$. Likewise, the blue circle with $n = 2$ is the secondary radius of the celestial sphere (cf. (25)) and its inverse, blue circle with $n = -2$, is the Kepler radius r_k (19–20). The 3-dimensional view (right panel), when viewed from the top, shows the discrete vanishing orbit of Earth in perspective and when viewed from the bottom indicates the stepwise increase of the radius of the celestial sphere.

with a radial field of view equivalent to β^3. Stellar aberration correction in the context of an infinite-radius celestial sphere overcorrects the position of the stars. It causes the fixed stars to have positive parallax and inadvertently make them nearby stars. Instead, abandoning corrective measures and recognizing the finite-radius celestial sphere, stars or nebulae exhibiting positive parallax above 0.002 arcsec are within 1 602 light-years of Earth, and those with less than 0.002 arcsec but above 0.2 μarcsec are within 16 million light-years (4.9 Mpc) from Earth.

7 Solar barycentre precession

With respect to Earth, motion of the other planets add additional aberration of the fixed stars by the wobbling Sun because the solar system barycentre is composed by the individual barycenters for each planet*. Sun and planet share a common celestial sphere because the angular velocity, centered on the barycentre of the Sun and planet orbits, is identical, but the orbital velocities of Sun and planet are different and so are the subtending angles that define stellar aberration when viewed from the Sun and planet, respectively. Table 1 (rows 3–6) tabulates specific planetary-based values of Sun's offset to and orbital velocity around the individual barycentre. Major contributors to affect the common barycentre are Jupiter, Saturn, Neptune and Uranus in that order. In return, orbits of planetary celestial spheres change with the periods of the outer planets adding offsets to stellar aberration. Focusing on the effect of Jupiter has on each of the planetary celestial spheres, the torque produced by Jupiter on the Sun adds a wobble with a period of 11.9 Earth-years. The stellar aberration from the Sun orbit around the Sun-Jupiter barycentre equals a subtending angle of 0.00858 seconds of an arc (Table 1, row 7) and becomes an independent component of stellar aberration as observed on Earth. Saturn, Neptune, Uranus contribute significantly and affect the solar system barycentre radius, giving rise to a precession of the celestial sphere coordinates, or in other words, the counterclockwise precession of the solar system barycentre will be "written" at each and

*en.wikipedia.org/wiki/Barycentric_coordinates_(astronomy)

every point of the coordinate system. The barycentre-induced wobble of the Sun might explain S-02's motion centered on Sagittarius A* that has currently a period of about 15 years, has an inclination similar to the ecliptic with respect to the galactic centre and matches the Sun's current orbit and period around the solar system barycentre. The year-by-year (Earth year) subtending angle of the apparent orbit of S-02 as seen from Earth matches the 0.00858 seconds of an arc (Table 1, row 7). Additional contributions are caused by Saturn and Uranus because they are currently located relatively close to Jupiter's position. S-02 is known to rotate in a clockwise direction and is consistent with the notion that Jupiter lags Earth's motion and Earth is the reference against which Jupiter will have the clockwise direction as has the Sun. We note that there are other stars revolving Sagittarius A* with significant longer periods and different inclinations, not associated with the solar barycentre or the ecliptic; this does not take away a possible explanation for S-02's motion.

8 Geometric inversions about an inversion circle

The tracing out of multiple imaginary orbits at discrete distances (Fig. 5), according to

$$C_n = \beta^{-n} R, \tag{21}$$

suggests also considerations when $n \leq 0$. If $n = 0$ it follows that the celestial sphere radius C_0 equals the orbital radius R and (7) becomes (cf. (6))

$$OQ = R\cos\theta \pm R\cos\theta, \tag{22}$$

because $\theta = \phi$. This scenario is the equivalent of the fictitious annual circulation (negative parallax) of the Sun through the zodiac. When $n < 0$, and by generalizing (19), (cf. (21)) we get

$$r_k = \beta^{2+n} C_n \tag{23}$$

celestial sphere radii less than the orbital radius. Since the vorticity, i.e. the velocity field, is determined by the angular velocity of the orbit, the tangential velocity of the celestial sphere coordinates will be less than the orbital velocity. Defining u_C as the tangential velocity of the coordinates and Ω as the angular velocity of the planetary orbit and utilizing (21) for $n \in N$, and defining u'_C when n is negative, we get

$$\begin{aligned} u_C &= \Omega \times C_n = \Omega \times \beta^{-n} R = \beta^{-n} v \\ u'_C &= \Omega \times C'_n = \Omega \times \beta^{n} R = \beta^{n} v. \end{aligned} \tag{24}$$

These equations suggest geometric inversion of points on the circle C_n to their inverse points on circle C'_n with respect to an inversion circle with inversion centre E and inversion radius R. The points on circles C_n and C'_n obey $C_n C'_n = R^2$, the defining feature of circle inversion. Furthermore, the radius $C'_2 = \beta^2 R$, identical to the Kepler radius r_k (19), has its inverse

$$r'_k = \beta^{-2} R \tag{25}$$

as defined by C_2. The tangential velocities of points and their inverse points (the coordinates) obey

$$u_C\, u'_C = v^2 \Leftrightarrow \frac{u'_C}{v} = \frac{v}{u_C}. \tag{26}$$

The Sun's position O and its inverse O', where $O' = O$, are located on the inversion circle. The line-of-sight from the inversion centre E (Fig. 4) to point Q on C_1 harbors Q' on C'_1 (5). In other words, when n is positive, the fictitious orbit is located at the radial distance C_n; when n is negative, C'_n is the radius of the vanishing fictitious orbit in perspective (Fig. 5).

9 Velocity field of the orbit of the Sun

Diurnal and annual motion of the heavens led to paradigm reversals, leading to the first and second motions of the Earth. The third motion of Earth, now known as the axial precession, was, in ancient and medieval times, ascribed to the precession of the equinoxes, a westward motion of the equinoxes along the ecliptic relative to the fixed stars in a cycle of 25 776 years. Precession affected all fixed stars as well as the apparent position of the Sun relative to the backdrop of the stars. The heavens slowly regress a full 360° through the zodiac at the rate of 50.3 seconds of arc per year*. Also, other ancient astrologers discovered that the equinoxes "trepidated", particularly along an arc of 46°40' [6], i.e. twice the obliquity of the equinoxes, in one direction and a return to the starting point, resembling how stellar aberration was discovered [2]. The precession and the trepidation appear to be two aspects of the same to-be-proposed frame dependent circulation (Fig. 6), which contrasts Newton's axial precession involving gravitational forces of the Sun and the Moon. Envisioning the Sun orbiting a centre counterclockwise with a period of 25 776 years, with the axis of the Earth in a fixed position (Fig. 6) and noting (18), the radius of the celestial sphere of the Sun becomes 4 102 light-years. Because the equinoctial aberration of the stars is 23.4°, β equals 0.3971, we get an orbital velocity of 119 062 km/s. The radius of the orbit (cf. (21)) is 491.5 pc, or 1 602 light-years and Kepler's radius (19) equals 75.0 pc, which translates to 1.57×10^{15} solar masses at the centre of rotation, vastly exceeding (by 4 magnitudes) current estimates of the Milky Way. The inclination of the zodiacal plane with respect to the invariable plane of the Milky Way galaxy may suggest that the centre of the precession of the equinoxes is not Sagittarius A*. While these values are staggering, concerning or exciting, there may be truth from ancient recordings.

10 Doppler shift measurements from a non-inertial reference frame

Spectroscopic measurement of electromagnetic radiation requires knowledge of Earth's motion, which includes not only the first and second motions, but also the third (Section 9) and

*en.wikipedia.org/wiki/Axial_precession

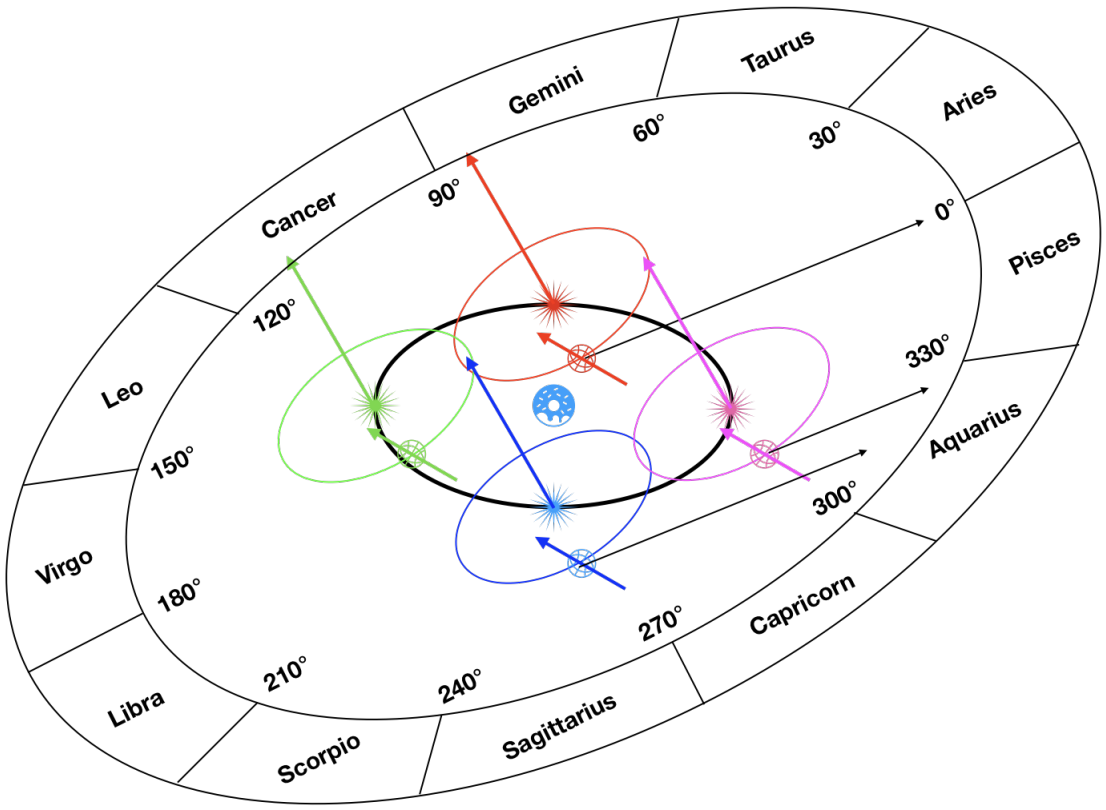

Fig. 6: **Stellar aberration by the precession of the equinoxes.** The orbit of Earth around the Sun is shown at four different positions of the Sun in its orbit about the equinoctial center shown as a blue-colored donut shaped symbol. The color coded arrows centered on Earth depicts the north celestial pole of Earth's celestial sphere. The color coded arrows centered on the Sun defines the north celestial pole of the celestial sphere of the Sun. It is assumed that the orbit of the Sun has an obliquity of 30°. Sun's orbit causes stellar aberration with an angular distance of 23.4°, causing equinoctial precession aberration at the vernal equinox. The line-of-sight in the direction of the first point of Aries (0°) is shown by a black arrow. Equinoctial aberration occurs in all directions of the line-of-sight similar to the oscillatory motion of the annual stellar aberration caused by Earth's motion around the Sun.

higher motions. The transformations (13), according to matrix $\mathbf{L}_\odot$ (16), transform the arguments of a sinusoidal wave,

$$\omega t' = k\mathbf{r}', \tag{27}$$

where ω is the angular frequency and k is the angular wavenumber of the waveform, to

$$\omega \sec\phi \left(t - \mathbf{r}c^{-1}\sin\phi\right) = k\sec\phi\,(\mathbf{r} - ct\sin\phi)\,. \tag{28}$$

Because $\omega k^{-1} = c$, the above identity after rearranging becomes

$$\omega t \sec\phi\,(1+\sin\phi) = k\mathbf{r}\sec\phi\,(1+\sin\phi)\,. \tag{29}$$

We note that the velocity u of the wave is not affected because

$$u = \frac{\mathbf{r}}{t} = \frac{\omega\sec\phi\,(1+\sin\phi)}{k\sec\phi\,(1+\sin\phi)} = c, \tag{30}$$

which is the defining feature of the Lorentz matrix. The transformation changes the waveform by $\sec\phi(1+\sin\phi)$ in the frequency and wavenumber domains with $\sin\phi$ representing the direction cosine, i.e. the line-of-sight. This Doppler effect, alternatively expressed in terms of $\sin\theta$ (7–9) along the line-of-sight relative to the position of the planet in its orbit, yields a shift z by

$$z + 1 = \sec\phi(1+\sin\phi) = \sqrt{\frac{1+\beta\sin\theta}{1-\beta\sin\theta}}\,. \tag{31}$$

Eq. (31) is applicable to any circular motion obeying Kepler's law, such as the Global Position System that sends radio signals. Receivers on Earth will detect a changing Doppler shift depending on the line-of-sight ϕ. Another example tied to (31) is the meaning of a gravitational redshift, which is the equivalent of traversing the Kepler circulation encountering an ever decreasing vorticity with increasing radial distance (19). The cosmological redshift, representing the expansion of the coordinate system, allows speeds greater than the speed of light, where v represents the speed of expansion, not of motion. However, when the ratio of frequencies is equated with

(peculiar) motion v/c,

$$z + 1 = \frac{\omega_{receiver}}{\omega_{source}} = \frac{v}{c} + 1, \tag{32}$$

and noting the last reported value $z = 11.1$ from galaxy GN-z11, the matrix identities (16,17) and their interpretation (Section 4) do not indicate incompatibility with the Doppler effect. Hence, the expanding universe is likely to be illusionary. In the context of Earth and its celestial sphere being subject to a multitude of circular motions and considering (31) that has two unknowns, θ and β, they may indicate novel periodic changes of the Doppler shift. It is possible that a multitude of orbits would temporally increase Earth's nominal velocity to go beyond the speed of light. The detection of frequency shifts of the order of GN-z11, using $\mathbf{L}_\odot$ (16), may indicate this and if assuming the Milky Way has an orbital velocity close to the speed of light and assuming $\sin\theta = 1$, we have $\beta = 0.984$ for $z = 11.1$. So (32) becomes (cf. (31)),

$$\frac{\omega_r^2}{\omega_s^2} = \frac{1 + \beta\sin\theta}{1 - \beta\sin\theta} \Rightarrow \beta\sin\theta = \frac{\omega_r^2 - \omega_s^2}{\omega_r^2 + \omega_s^2}\,. \tag{33}$$

Stars and nebulae beyond the Milky Way may sometimes shine very bright or become very dim at the firmament if Earth obtains a nominal speed equal to the speed of light. Beyond the speed of light the square root of (31) produces an imaginary, inverse result. Geometric inversion (cf. (24)) means passing the luminal barrier, such that

$$\frac{u}{c} = \frac{c}{u'} \Rightarrow uu' = c^2, \tag{34}$$

where $u \leq c$ and $u' \geq c$. We get

$$\frac{\omega_r^2}{\omega_s^2} = \frac{u' + c\sin\theta}{u' - c\sin\theta} = \frac{c^2/u + c\sin\theta}{c^2/u - c\sin\theta} = \frac{c + u\sin\theta}{c - u\sin\theta}\,, \tag{35}$$

which is identical to (31). The waveform emanating from a body with velocity u' is not different from a waveform emanating from a body with velocity u and the velocity of our galaxy with respect to the speed of light might be either u or u'. We might not know, but acknowledging frame-dependent induced negative parallaxes may shed further insight in what the universe looks like.

11 Conclusions

Illusion, paradox and true-to-reality phenomena are intertwined in our current worldview, governed by an infinite-radius celestial sphere and merged with the theory of relativity that suggests that space and time are not absolute. The human perception of the third dimension of the universe, be it relativistic or classical in nature, suffers from reversed perspective. The transformations to detect the location of a point by light is governed by the set of the Lorentz **L**, the Galilean **G** and the light retardation **T** matrices. Vice versa, light signals from objects are transformed by premultiplying the Lorentz matrix with the inverse of the light retardation matrix to obtain the Galilean transform. The finite-radius celestial sphere, providing true-to-reality perception, changes the sign of the direction of stellar aberration and therefore parallax of the coordinate system. This recognition may explain co-rotating satellite systems such as a large-scale structure of the universe or the cosmic web. Another large structure of the universe is envisioned based on a fixed Earth axis and a solar orbit with a 1 602 light-year radius about an intragalactic centre causing the precession of the equinoxes with an equinoctial stellar aberration of 23.4°. The infinite-radius celestial sphere is a relic of ancient times when Earth was considered the centre of the universe. When the second motion of Earth became main stream physics, it should have been accompanied with a finite-radius celestial sphere. It did not because stellar aberration was not discovered until 300 years ago.

Received on July 4, 2020

References

1. Purves D., Andrews T. J. The perception of transparent three-dimensional objects. *Proc. Natl. Acad. Sci. USA*, 1997, v. 94, 6517–6522.
2. Bradley J. A Letter from the Reverend Mr. James Bradley Savilian Professor of Astronomy at Oxford, and F.R.S. to Dr. Edmond Halley Astronom. Reg. &c. Giving an Account of a New Discovered Motion of the Fix'd Stars. *Philos. Trans. R. Soc.*, 1729, v. 35, 637–661.
3. Einstein A. Zur Elektrodynamik bewegter Körper. *Ann. Phys.*, 1905, v. 322, 891–921.
4. Lee J. H., Pak M., Song H., Lee H. R., Kim S., Jeong H.Mysterious Coherence in Several-megaparsec Scales between Galaxy Rotation and Neighbor Motion. *Astrophys. J.*, 2019, v. 884, 104.
5. Newcomb S. A Compendium of Spherical Astronomy. Macmillan Co., New York,,, 1906 p. 90.
6. Pingree D. Precession and Trepidation in Indian Astronomy before A.D. 1200. *J. Hist. Astron.*, 1972, v. 3, 27–35.